Analysis and Design of High Power Interleaved Boost Converters for Fuel Cell Distributed Generation System

Haiping Xu, Ermin Qiao, Xin Guo, Xuhui Wen, Li Kong,
Inst. of Electrical Engineering (IEE), Chinese Academy of Sciences (CAS),
P O.box 2703, Beijing, P.R.China, 100080

***Abstract*-This article proposes a novel topology of high power Interleaved Boost Converter for Fuel Cell. With thorough analysis of the operating principle of the converter, eight equivalent sub-circuits are described. According to the waveforms of the inductor current, the operation modes of the converter are classified to six kinds, including CCM (continuous conducting mode) and DCM (discontinuous conducting mode), and the uniform state–space averaged model of the converter in CCM and DCM are developed. Based on the transfer function, the two-loop controllers are designed, and a prototype of 150 kW Converter that is controlled by DSP-320F2407 is constructed. The volume and weight of the proposed converter are decreased 1/3 than conventional converter and the efficiency is over 97%. The experimental results show that the converter has excellent electrical characteristics, and it can be applied in the Fuel Cell Distributed Generation system.**

I. INTRODUCTION

Distributed generation (DG) technologies can provide energy solutions to some customers that are more cost-effective, more environmentally friendly, or provide higher power quality or reliability than conventional solutions. The application of fuel cell technologies to DG portends the most significant advancement in energy efficiency, conservation, and environmental protection. Proton exchange membrane Fuel Cell (PEMFC) are rapidly developed as the primary power source in movable power supplies and DG. The voltage of PEMFC stack decreases largely as the load current increase, and the voltage increases as the temperature increase at the same current. Therefore, DC–DC converter is needed to provide a constant voltage to other electrical apparatus. Besides, DC–DC converter plays an important role in the Energy Management System.

In this paper, A High Power Interleaved Boost Converter for Fuel Cell is proposed, the operating principle of the converter is analyzed thoroughly, and the uniform state–space averaged model of the converter in CCM (continuous conducting mode) and DCM (discontinuous conducting mode) is developed. Using DSP-320F2407 as main controller, a prototype of 150 kW DC-DC Converter is designed and some of the experimental results are discussed.

II. THE PRINCIPLE OF INTERLEAVED BOOST CONVERTER

In order to achieve the requirement of small volume, light weight, and reliable properties, a High Power Interleaved Boost Converter is constructed, as shown in fig 1.

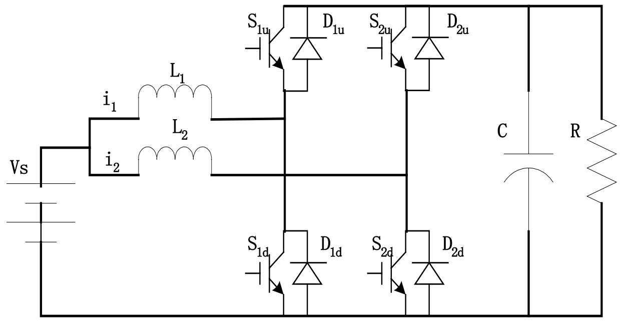

Fig 1. The topology of the Interleaved Boost Converters

The principle of Interleaved Boost Converter as follows: each phase is a BOOST/BUCK DC-DC Converter, which is composed of a bridge of power switches and storage energy inductor. When S1u=S2u=OFF, S1d and S2d switch on and off, the system work in the BOOST mode, shown in Table 1.

Tab 1. The state of the power device in BOOST mode

S1u=OFF	S2u=OFF	D1u= ON / OFF	D2u= ON / OFF
S1d= ON / OFF	S2d= ON / OFF	D1d=OFF	D2d=OFF

From the table 1, we can see that in Boost mode, only the power devices (S1d,S2d,D1u,D2u) have switching commutation, the power devices (S1u,S2u,D1d, D2d) have no commutation. The power switches S1d and S2d have 180-degree phase difference of driving pulses in a cycle. The current fluctuation of input power supply is reduced greatly because the two 180-degree phase difference inductor currents minify the fluctuation of each other [1] [4]. In one switching cycle Ts, considering the commutation of power switches and diodes (S1d,S2d,D1u,D2u), there have eight kinds of running states, as shown in Table 2.

Tab 2. The eight kinds of running states in interleave BOOST mode

	S1d=on	S2d=on	D1u=on	D2u=on
S1d=on	State 2	State 7	*	State 1
S2d=on	State 7	State 5	State 4	*
D1u=on	*	State 4	State 3	State 8
D2u=on	State 1	*	State8	State 6

According to Tab 2, The converter have eight equivalent sub-circuits of state 1~state 8，as shown in Fig 2.

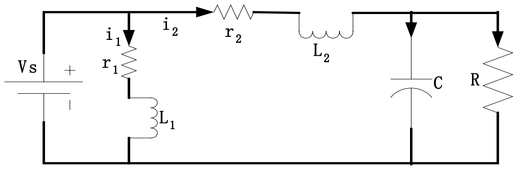

Fig 2a. The equivalent sub-circuits of state 1

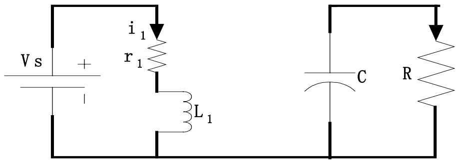

Fig 2b. The equivalent sub-circuits of state 2

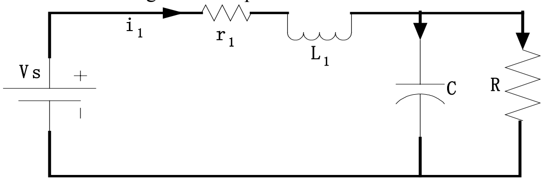

Fig 2c. The equivalent sub-circuits of state 3

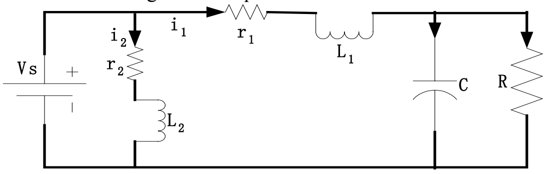

Fig 2d. The equivalent sub-circuits of state 4

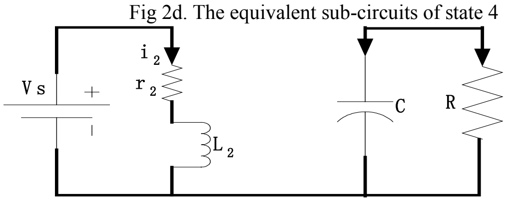

Fig 2e. The equivalent sub-circuits of state 5

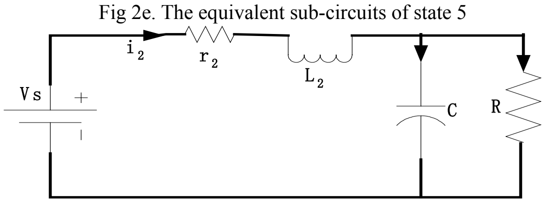

Fig 2f. The equivalent sub-circuits of state 6

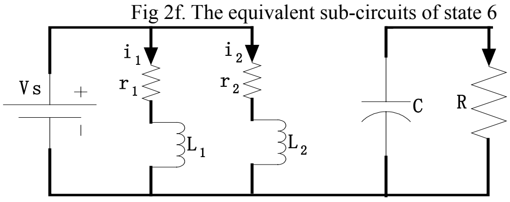

Fig 2g. The equivalent sub-circuits of state 7

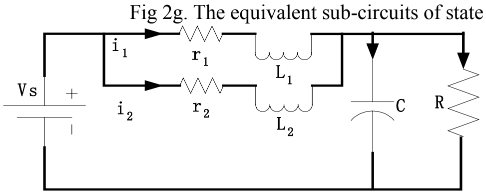

Fig 2h. The equivalent sub-circuits of state 8

III. STATE-SPACE AVERAGED SYSTEM MODEL

The state space equations are separately established according to the equivalent circuits in Fig 2. Supposing i_1, i_2, V_c as the state variables and V_s as the variable of the input voltage and V_0 as the variable of the output voltage. The state equation of the converter is ：

$$\dot{X} = A_n X + B_n V_S \text{.......... ....} during \text{ ...} d_n * T_s$$
$$V_0 = C_n X \qquad \dots (1)$$
$$n = 1,2,3,4,5,6,7,8$$

$$A_1 = \begin{bmatrix} -\frac{r_1}{L_1} & 0 & 0 \\ 0 & -\frac{r_2}{L_2} & -\frac{1}{L_2} \\ 0 & \frac{1}{C} & -\frac{1}{RC} \end{bmatrix}, \text{....} B_1 = \begin{bmatrix} \frac{1}{L_1} \\ \frac{1}{L_2} \\ 0 \end{bmatrix}, \text{....} C_1 = \begin{bmatrix} 0 & 0 & 1 \end{bmatrix}$$

$$.A_2 = \begin{bmatrix} -\frac{r_1}{L_1} & 0 & 0 \\ 0 & 0 & 0 \\ 0 & 0 & -\frac{1}{RC} \end{bmatrix}, \text{....} B_2 = \begin{bmatrix} \frac{1}{L_1} \\ 0 \\ 0 \end{bmatrix}, \text{....} C_2 = \begin{bmatrix} 0 & 0 & 1 \end{bmatrix}$$

$$.A_3 = \begin{bmatrix} -\frac{r_1}{L_1} & 0 & -\frac{1}{L_1} \\ 0 & 0 & 0 \\ \frac{1}{C} & 0 & -\frac{1}{RC} \end{bmatrix}, \text{....} B_3 = \begin{bmatrix} \frac{1}{L_1} \\ 0 \\ 0 \end{bmatrix}, \text{....} C_3 = \begin{bmatrix} 0 & 0 & 1 \end{bmatrix}$$

$$.A_4 = \begin{bmatrix} -\frac{r_1}{L_1} & 0 & -\frac{1}{L_1} \\ 0 & -\frac{r_2}{L_2} & 0 \\ \frac{1}{C} & 0 & -\frac{1}{RC} \end{bmatrix}, \text{....} B_4 = \begin{bmatrix} \frac{1}{L_1} \\ \frac{1}{L_2} \\ 0 \end{bmatrix}, \text{....} C_4 = \begin{bmatrix} 0 & 0 & 1 \end{bmatrix}$$

$$.A_5 = \begin{bmatrix} 0 & 0 & 0 \\ 0 & -\frac{r_2}{L_2} & 0 \\ 0 & 0 & -\frac{1}{RC} \end{bmatrix}, \text{....} B_5 = \begin{bmatrix} 0 \\ \frac{1}{L_2} \\ 0 \end{bmatrix}, \text{....} C_5 = \begin{bmatrix} 0 & 0 & 1 \end{bmatrix}$$

$$.A_6 = \begin{bmatrix} 0 & 0 & 0 \\ 0 & -\frac{r_2}{L_2} & -\frac{1}{L_2} \\ 0 & \frac{1}{C} & -\frac{1}{RC} \end{bmatrix}, \text{....} B_6 = \begin{bmatrix} 0 \\ \frac{1}{L_2} \\ 0 \end{bmatrix}, \text{....} C_6 = \begin{bmatrix} 0 & 0 & 1 \end{bmatrix}$$

$$.A_7 = \begin{bmatrix} -\frac{r_1}{L_1} & 0 & 0 \\ 0 & -\frac{r_2}{L_2} & 0 \\ 0 & 0 & -\frac{1}{RC} \end{bmatrix}, \text{....} B_7 = \begin{bmatrix} \frac{1}{L_1} \\ \frac{1}{L_2} \\ 0 \end{bmatrix}, \text{....} C_7 = \begin{bmatrix} 0 & 0 & 1 \end{bmatrix}$$

$$.A_8=\begin{bmatrix} -\frac{r_1}{L_1} & 0 & \frac{1}{L_1}\\ 0 & -\frac{r_2}{L_2} & \frac{1}{L_2}\\ \frac{1}{C} & \frac{1}{C} & -\frac{1}{RC}\end{bmatrix},....B_8=\begin{bmatrix}\frac{1}{L_1}\\ \frac{1}{L_2}\\ 0\end{bmatrix},....C_8=\begin{bmatrix}0 & 0 & 1\end{bmatrix}$$

AVERAGING: On the assumption that in one period T_s, the eight equivalent sub-circuits will run d_n*T_s respectively. The state-spaced equations of eight sub-circuits are time weighted and averaged over the switching period T_s. So the state–space averaged model of the whole system is:

$$\dot{X}=(A_1*d_1+A_2*d_2+A_3*d_3+A_4*d_4+A_5*d_5+A_6*d_6+A_7*d_7+A_8*d_8)X$$
$$+(B_1*d_1+B_2*d_2+B_3*d_3+B_4*d_4+B_{15}*d_5+B_6*d_6+B_7*d_7+B_8*d_8)V_S$$
$$V_0=(C_1*d_1+C_2*d_2+C_{13}*d_3+C_4*d_4+C_5*d_5+C_6*d_6+C_7*d_7+C_8*d_8)X \qquad \text{...... (2)}$$

The state matrix A，B and C are：

$$A=\begin{bmatrix} \frac{r_1(d_1+d_2+d_3+d_4+d_7+d_8)}{L_1} & 0 & \frac{(d_3+d_4+d_8)}{L_1}\\ 0 & \frac{r_2(d_1+d_4+d_5+d_6+d_7+d_8)}{L_2} & \frac{(d_1+d_6+d_8)}{L_2}\\ \frac{(d_3+d_4+d_8)}{C} & \frac{(d_1+d_6+d_8)}{C} & \frac{1}{RC}\end{bmatrix},$$

$$B=\begin{bmatrix}\frac{1}{L_1}(d_1+d_2+d_3+d_4+d_7+d_8)\\ \frac{1}{L_2}(d_1+d_4+d_5+d_6+d_7+d_8)\\ 0\end{bmatrix}......C=\begin{bmatrix}0 & 0 & 1\end{bmatrix}$$

The interleaved Boost converter can operate in CCM or DCM, and the inductor current waveforms of the converter have six kinds of shape according to the duty of the PWM pulse (D), as shown in Fig 3.

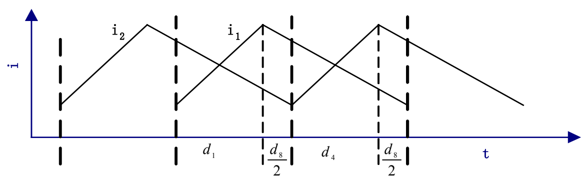

Fig 3a. The current of the two inductors, CCM (D<0.5)

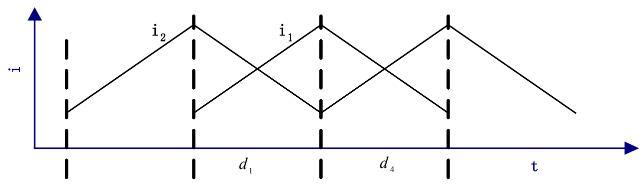

Fig 3b. The current of the two inductors, CCM (D=0.5)

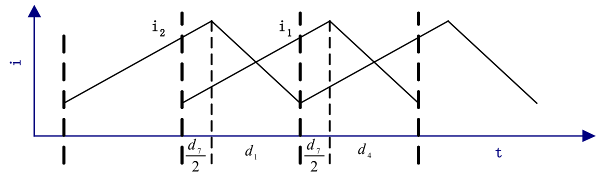

Fig 3c. The current of the two inductors, CCM (D>0.5)

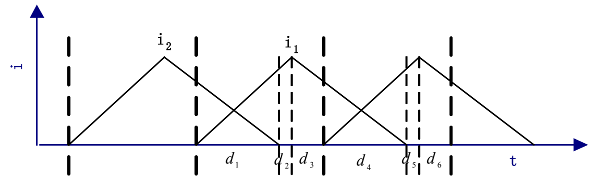

Fig 3d. The current of the two inductors, DCM (D<0.5)

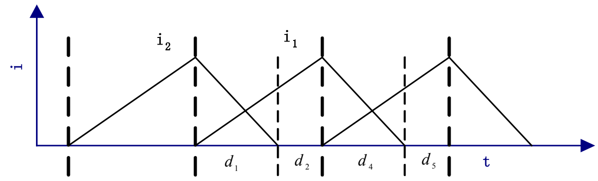

Fig 3e. The current of the two inductors, DCM (D=0.5)

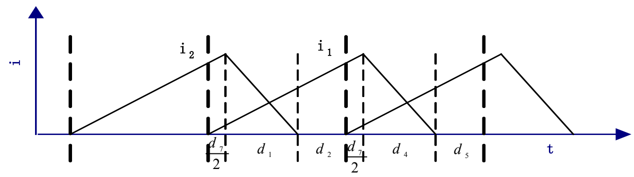

Fig 3f. The current of the two inductors, DCM (D>0.5)

Define: D, rising time of the inductor current. D_p, Falling time of the inductor current.

1) CCM (D<0.5)：The converter works in state 1, state 4 and state 8. Because there are two times of state 8 in one period, the running time of the each state 8 is 1/2* d_8， as shown in Fig 3a.

2) CCM (D=0.5)：The converter works in state 1, state 4, as shown in Fig 3b.

3) CCM (D>0.5)：The converter works in state 1, state 4 and state 7. Because there are two times of state 7 in one period, the running time of the each state 7 is 1/2* d_7， as shown in Fig 3c.

4) DCM (D<0.5)：The converter works in state 1~ state 6, as shown in Fig 3d.

5) DCM (D=0.5)：The converter works in state 1, state 2, state 4 state 5, as shown in Fig 4e.

6) DCM (D>0.5)：The converter works in state 1, state 2, state 4 state 5 and state 7. Because there are two times of state 7 in one period, the running time of the each state 7 is

1/2* d_7 , as shown in Fig 3f.

On the assumption that the two phase circuits is symmetrical, so, $L_1 = L_2$, $r_1 = r_2$, $d_1 = d_4$, $d_2 = d_5$, $d_3 = d_6$.

The uniform state–space averaged model of the whole system in CCM and DCM will be gained.

CCM:

$$.A = \begin{bmatrix} -\frac{r_1}{L_1} & 0 & -\frac{(1-D)}{L_1} \\ 0 & -\frac{r_2}{L_2} & -\frac{(1-D)}{L_2} \\ \frac{(1-D)}{C} & \frac{(1-D)}{C} & -\frac{1}{RC} \end{bmatrix},$$

$$B = \begin{bmatrix} \frac{1}{L_1} \\ \frac{1}{L_2} \\ 0 \end{bmatrix}, \ldots\ldots\ldots \ C = [0 \quad 0 \quad 1]$$

DCM:

$$.A = \begin{bmatrix} -\frac{r_1(D+D_P)}{L_1} & 0 & -\frac{D_P}{L_1} \\ 0 & -\frac{r_2(D+D_P)}{L_2} & -\frac{D_P}{L_2} \\ \frac{D_P}{C} & \frac{D_P}{C} & -\frac{1}{RC} \end{bmatrix},$$

$$B = \begin{bmatrix} \frac{1}{L_1}(D+D_P) \\ \frac{1}{L_2}(D+D_P) \\ 0 \end{bmatrix}, \ldots\ldots\ldots \ C = [0 \quad 0 \quad 1]$$

STEADY-STATE:

$$X = -A^{-1}BV_s$$

$$V_0 = -CA^{-1}BV_S \quad \ldots\ldots\ldots\ldots\ldots\ldots\ldots\ldots (3)$$

The steady characteristics of the converter are as follows.

CCM:

$$M = \frac{V_0}{V_s} = \frac{1}{1-D}$$

$$I_1 = I_2 = \frac{V_S}{2R(1-D)^2}$$

$$V_0 = \frac{V_S}{1-D}$$

DCM:

$$M = \frac{V_0}{V_s} = 1 + \frac{D}{D_P}$$

$$I_1 = I_2 = \frac{D + D_P}{2RD_P^2} V_S$$

$$V_0 = \frac{D + D_P}{D} V_S$$

$$D_P = \frac{K(1 + \sqrt{1 + 4D^2 / K}}{2D}$$

$$K = \frac{L}{RT_S}$$

IV. THE DESIGN OF THE CONTROLLER

A. System transfer function

The dynamic characteristics of the converter: when $r_1 = r_2 \approx 0$, the order of the state equation will be descend to two.

CCM:

$$.A = \begin{bmatrix} 0 & -\frac{(1-D)}{L} \\ \frac{(1-D)}{C} & -\frac{1}{RC} \end{bmatrix}$$

$$B = \begin{bmatrix} \frac{1}{L} \\ 0 \end{bmatrix}, \ldots\ldots\ldots \ C = [0 \quad 1]$$

DCM:

$$.A = \begin{bmatrix} 0 & -\frac{D_P}{L} \\ \frac{D_P}{C} & -\frac{1}{RC} \end{bmatrix}$$

$$B = \begin{bmatrix} \frac{1}{L}(D+D_P) \\ 0 \end{bmatrix}, \ldots\ldots\ldots \ C = [0 \quad 1]$$

Considering the effect of the control variable D, the state-space averaged equation is described to,

$$\dot{X} = F(x, v_s, d) \ , \quad \ldots\ldots\ldots\ldots\ldots\ldots\ldots\ldots \ldots\ldots (5)$$

Then, the small signal model of the converter is

$$\dot{\hat{x}} = A'\hat{x} + B'\hat{v}_s + K\hat{d} \quad \ldots\ldots\ldots \ldots\ldots (6)$$

$$A' = \frac{\partial F}{\partial x}, B' = \frac{\partial F}{\partial v_s}, K = \frac{\partial F}{\partial d}$$

The control to state variable transfer functions is:

$$\frac{\hat{x}}{\hat{d}} = (sI - A')^{-1} K \quad \ldots\ldots\ldots\ldots\ldots\ldots\ldots\ldots\ldots (7)$$

$$Gid(s) = \frac{RCV_0 * s + 2V_0}{RLC * s^2 + L * s + RD_p^2} \quad \ldots\ldots\ldots\ldots\ldots (8)$$

$$Gvd(s) = \frac{-LV_0 / D_p * s + V_0 RD_p}{RLC * s^2 + L * s + RD_p^2} \quad \ldots(9)$$

B. Design of Digital Controller

Based on the transfer function above, the BODE PLOT can be drawn and the digital controller can be designed. The control system of this converter is a double closed-loop, outer voltage loop and inner current loop, fully digitalized with DSP, The dual-loop controller is shown in Fig 4.

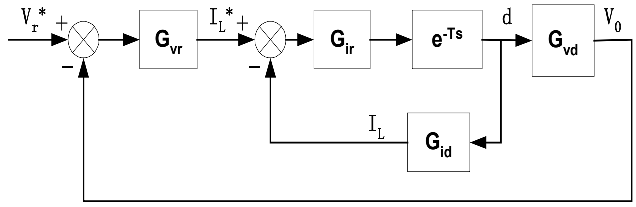

Fig 4. The dual-loop controller of the converter

The loop gains for inner current loop and outer voltage loop can be expressed as:

$$H_i(s) = G_{ir} * G_{id} * e^{-Ts} \quad \ldots\ldots\ldots\ldots\ldots\ldots\ldots\ldots\ldots. (10)$$

$$H_v(s) = \frac{G_{vr} * G_{ir} * e^{-Ts} * G_{vd}}{1 + H_i} \quad \ldots(11)$$

In a two-loop BOOST system, the current compensator is designed for good loop dynamics， and the voltage compensator is designed for the desired crossover frequency and phase margin.

V. Experimental Result

Based on the analysis above, using DSP-320F2407 as main controller, a prototype of a fully digitalized Interleaved Boost Converter was constructed with its basic technical specification as follows: P=150 kW, 250 V $\le V_s \le$450 V, V_0=584 V. The proposed converter weigh 50Kg and hold 50L，which lessen one third of the volume and weight than single phase BOOST converter, moreover, the fluctuation of current is less than 10 %. The photo of the converter is shown in Fig 5.

Fig5：the photo of the interleave Boost converter

Figures.6 are the waveforms of the Interleaved Boost Converter working at 75kW. Fig 6a are the driving signals of the two phase IGBT switches, which have the equal duty and have 180-degree phase difference. Fig 6b are the waveforms of its output voltage and current, which shows that the voltage fluctuation is less than 1%. Fig 6c are the waveforms of the Inductor current of one phase and output voltage, it can be seen that the converter run at critical state between CCM mode and DCM mode. Fig 6d are the waveforms of voltage and current of inductor at half load. Fig 6e are the waveforms of two phases Inductor current at half load. Fig 6f are the waveforms of Inductor current and input current. The ripple coefficient of the input current is less than 10%. Fig 7 is the waveforms of output voltage and current when the system is soft started and stopped, in which we can see that the soft start period is 2s. Fig 8 is the system efficiency curve, which indicates that the whole efficiency is about 95~98% ，and the efficiency is over 97% when the output power is large than the half of rated power .

The related parameters of the oscillograph are: voltage—200V/div, current—100A/div.

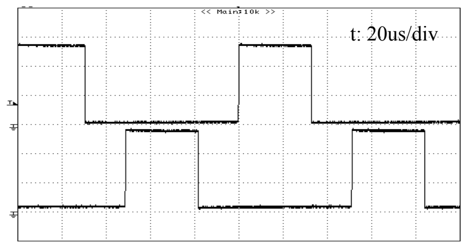

Fig 6a：Drive signals of two-phase IGBT switches

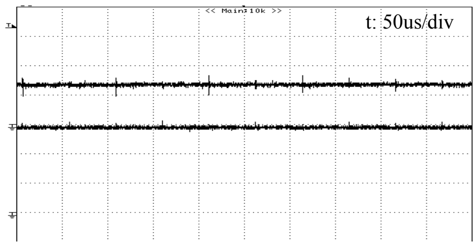

Fig 6b：Output current (upper) and output voltage (lower) at 75kW

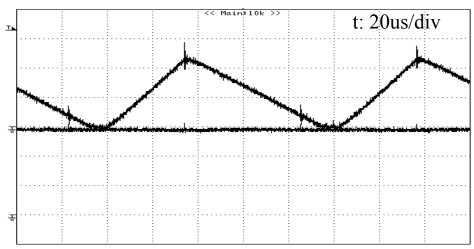

Fig 6c：Inductor current (upper) and output voltage (lower) at 75kW

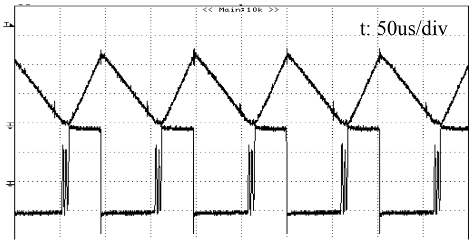

Fig 6d：Inductor current (upper) and voltage (lower) at 75kW

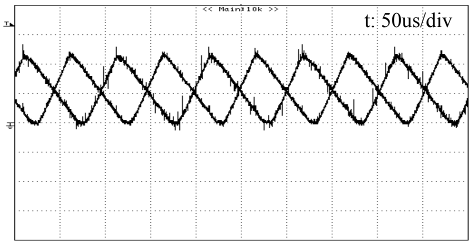

Fig 6e：two phase Inductor current at 75kW

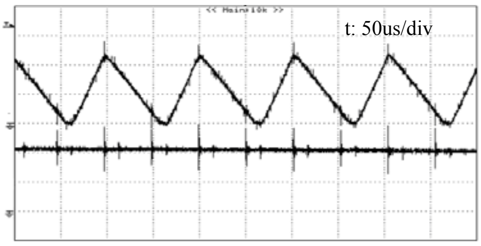

Fig 6f：Inductor current (upper) and input current (lower) at 75kW

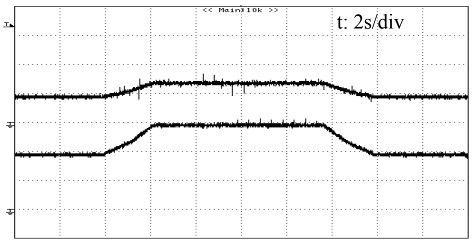

Fig 7：Output current (upper) and voltage (lower) at soft start/stop

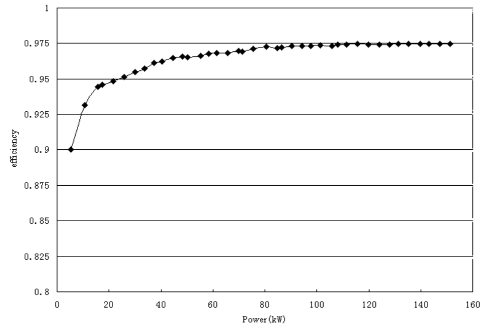

Fig 8：the system efficiency curve

VI. CONCLUSIONS

In conclusion, the proposed High Power Interleaved Boost Converter for Fuel Cell and the state–space averaged model of the converter are verified by experiment. The efficiency of the Converter is over 97%, and the volume and weight are decreased 1/3 than conventional BOOST converter, moreover, the fluctuation of input current is less than 10 %. Owing to the digital control its dynamic and static characteristic is excellent. Therefore, the Interleaved Boost converter is suitable for Fuel Cell Distributed Generation system.

References

[1] David J. Perreault and Jhon G.Kassakian . “Distributed interleaving of paralleled power converters”. IEEE Trans. on Power Electronics, Vol. 9(4), pp.405-413, 1994

[2] Xudong Huang, Nergaard. T, Jih-Sheng Lai, Xingyi Xu, Lizhi Zhu. “A DSP based controller for high-power interleaved boost converters”. APEC '03, 9-13 Feb. 2003, Pages: 327 - 333 vol.1.

[3] X. Huang, X. Wang, J. Ferrell, T. Nergaard, J. Lai, X, Xu and L.Zhu, “Parasitic Ringing and Design Issues of High Power Interleaved Boost Converters,” in Conf. Rec. of IEEE Power Electronics Specialists Conference, 2002.

[4] Zang M.T., Jovanovic, M.M., and Lee F.C. “Analysis and evaluation of interleaving techniques in forward converters”. IEEE Trans. on Power Electronics, Vol. 13(4), pp.690-697, 1998.

[5] Haiping Xu, Li Kong, Xuhui Wen. “Fuel Cell power system and high power DC-DC converter”. IEEE Trans. on Power Electronics, Vol. 19(5), pp.1250-1255, 2004